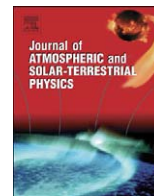




Contents lists available at ScienceDirect

Journal of Atmospheric and Solar-Terrestrial Physics

journal homepage: www.elsevier.com/locate/jastp

The PFISR IPY observations of ionospheric climate and weather

J.J. Sojka^{a,*}, M.J. Nicolls^b, C.J. Heinselman^b, J.D. Kelly^b^a Center for Atmospheric and Space Sciences, Utah State University, Logan, UT 84321, USA^b Sri International, Menlo Park, CA 94025, USA

ARTICLE INFO

Article history:

Accepted 7 January 2009

Available online 20 January 2009

Keywords:

Polar ionosphere observations
 Plasma temperature and density
 Ionosphere–magnetosphere interaction
 Ionosphere–atmosphere interaction
 Auroral ionosphere

ABSTRACT

The recently commissioned Poker Flat Incoherent Scatter Radar (PFISR) began a continuous operation measurement program for the duration of the International Polar Year (IPY). The IPY began on 1 March 2007 and is an 18-month period of intense polar study. PFISR began its IPY campaign on 1 March 2007 and this paper describes the first 10 months of observations. The PFISR IPY science goals revolve around distinguishing between ionospheric climate and weather variability, and to determine the relative role of geomagnetic weather from the magnetosphere versus that driven from the atmosphere below. This latter goal may well be aided by the fact that the IPY period is at solar minimum, a time when major geomagnetic activity occurrence should be minimized. However, as nature would have it once the IPY observations began it was found that geomagnetic activity was a recurrent feature lasting the entire 10 months being discussed here. The PFISR IPY database will also be used as a long-term fiducial data set against which ionospheric models are to be compared. Hence, this paper provides a documentation of the contents of the database. Case studies as well as statistical studies of how the ionospheric climate and weather can be separated are presented. A particular emphasis is placed upon the F-region ion temperature observations. These appear to provide a very direct measure of geomagnetic energy input to the ionosphere–thermosphere system. Examples are shown in which 150 K F-region ion temperature increases are associated with very moderate geomagnetic disturbances in which the daily average 3-h Kp is only 2.5.

© 2009 Elsevier Ltd. All rights reserved.

1. Introduction

The International Polar Year (IPY) began on 1 March 2007 and ran for approximately 18 months. An objective of the IPY is to quantify our present day understanding of the polar terrestrial environment from the sea through land up into the upper reaches of the atmosphere and through an 18-month period of focused and methodical observations that extend our knowledge of the polar regions. This paper describes one of these observational campaigns that uniquely specifies the polar ionosphere in ways not possible in the past. The observations in question are from the National Science Foundation's (NSF) Poker Flat Incoherent Scatter Radar (PFISR). PFISR is a new ISR, which was commissioned only 2 months before the start of IPY. The 450-MHz PFISR is a modern phased array system that transmits and receives over many thousands of elements, and as a result consists of no moving parts and no huge klystrons (consisting instead of distributed solid-state amplifiers). Indeed, with these two major ISR constraints removed, the PFISR can be operated remotely, and is operated remotely, with command sequences that can change research

modes essentially instantaneously. Because of the relatively low power of each transmit element, the entire system can be cold started and shut down safely without warm up periods or concerns about excessive switching. This provides a unique ISR capability that is central to the IPY observation program. PFISR's IPY contribution is to run "continuously" over the duration of IPY. To achieve this a PFISR ionospheric profile of electron density, electron temperature, ion temperature, and line-of-sight velocity is made at least once every 15 min along the Poker Flat magnetic field line (Sojka et al., 2007a).

The IPY period occurred during the solar minimum between the end of solar cycle 23 and beginning of 24. This provided a fortuitous geomagnetic condition in that large storms would be avoided and that in general geomagnetic activity would be low. Hence, the conditions were thought to be optimal for studies that focus on how the thermosphere and lower atmospheric regions affect the ionosphere at high latitudes. With hindsight no major geomagnetic storms occurred, however, recurrent periods on about a 10-day cycle of geomagnetic activity did occur. Each cycle had 2–5 days of significant activity. These cycles make identifying planetary wave effects from the atmosphere below rather difficult because of their similar periodicities. The PFISR IPY data set will become a fiducial reference mark for solar minimum. There is no earlier data set that is as comprehensive in observing the

* Corresponding author.

E-mail address: sojka@cc.usu.edu (J.J. Sojka).

ionosphere's key state parameters. These observations will now become the primary constraint on present day modeling of the high-latitude ionosphere. The physics-based models solve the transport equation moments; continuity, momentum, and energy (Schunk, 1996). The PFISR observations of profiles of electron density, electron temperature, ion temperature, and line-of-sight velocity provides almost complete constraints on these equations as plasma forms in the E-region or is transported in the F-region over Poker Flat, Alaska.

This paper presents a first look at the PFISR IPY data set as well as providing a climate weather sorting of these observations along with specific case-study events. In Section 2 the PFISR instrument will be described, while in Section 3 the specific PFISR IPY observational mode is described and a summary plot of data are shown. Section 4 provides a detailed view of the PFISR IPY database by concentrating on only four parameters; $N_m F_2$, $h_m F_2$, T_e at 300 km, and T_i at 300 km. Because of the “continuous” operation of the PFISR, events are captured in their entirety and two examples of this are shown in Section 4. The separation of weather (geomagnetic) and climate (season) is carried out statistically in Section 5. A brief discussion is found in Section 6 and the summary in Section 7 provides an invitation and challenge to the modeling community to participate in bringing the IPY ionospheric objectives to fruition.

2. PFISR IPY experiment description

The Poker Flat Incoherent Scatter Radar (PFISR) is located at the Poker Flat Research Range (65.13°N, 147.47°W) near Fairbanks, Alaska. The phased array nature of PFISR allows it to steer on a pulse-to-pulse basis. The modern design of the system allows it to be operated remotely with little to no monitoring and also allows for graceful degradation due to the use of solid-state amplifiers and modern electronics. The normal IPY mode is a single-look direction (up the local magnetic field line: azimuth -154.3° , elevation 77.5°), low duty cycle mode ($\sim 1\%$) that is designed for background characterization of the Poker Flat ionosphere. Augmented IPY modes include an additional two beams designed for characterization of the background electric field (e.g., Heinselman and Nicolls, 2008) and a full duty cycle mode operated for 24 h approximately every 2 weeks. PFISR operates in the low duty cycle IPY mode, which is the basis of this paper, for all times when the radar is not scheduled for other use. In addition, many modes are “IPY compatible” in that they run a similar set of pulse schemes with a beam pointed in the direction of the local magnetic field line—these data are automatically folded into the analysis presented here. Operations in the IPY or an IPY compatible mode constituted roughly $\sim 75\%$ of the available operating time from 1 March 2007 to 31 December 2007. Thus, the operations presented here, in conjunction with EISCAT Svalbard Radar IPY operations, constitute the most complete long-duration coverage for the better part of a year of any ISRs, ever.

The IPY mode consists of 2 sets of interleaved pulses: a 480 μ s (72 km) long pulse designed for F-region studies and a 30 μ s baud (4.5 km), 16 baud strong alternating code (Lehtinen and Haggstrom, 1987) designed for E-region work. Data are integrated for 15 min prior to fitting. The returned power has been calibrated using measured up- and down-shifted long pulse plasma line cutoff (Shownen, 1979) data over the same observation period, and in general the data are calibrated using a system constant approach (e.g., Evans, 1969). We estimate the returned power to be accurate within $\pm 5\%$ after calibration based on a statistical study of the variability of the system constant as a function of time. The system constant for PFISR is a function of the gain of the

system, which is dependent on the number of fully operational panels and thus the transmit power.

Incoherent scatter radars are able to infer electron and ion temperatures, electron densities, line-of-sight velocities, and under certain conditions other parameters such as composition directly by measuring the shape of the autocorrelation function of the medium (e.g., Dougherty and Farley, 1960). The statistics of the inferred parameters depend on the signal-to-noise ratio of the backscattered signal, which is a function of both the system and of the medium, and on the number of independent measurements integrated. For a typical daytime F-region ionosphere (long pulse measurements), and for PFISR operating in the low duty cycle IPY mode with 15 min integrations, temperatures can be inferred to within ~ 50 – 100 K, line-of-sight velocities can be inferred to within ~ 10 – 15 m/s, and densities can be inferred to within a statistical precision of $\sim 2\%$ (but are limited by the aforementioned source of calibration error). The range resolution of these measurements is limited by the pulse length (72 km), although products are computed every half pulse width after application of an appropriate summation rule.

3. PFISR IPY baseline operation mode

The data being acquired over the entire IPY period will represent the climate and weather of the ionosphere above the Poker Flat location. As an optimization decision this observation mode collects data along the local PFISR field line at a cadence no longer than 15 min. Since the IPY began on 1 March 2007, only about 60 days after the PFISR commissioning, the PFISR mode has been continually updated to extend its data collection. The cadence is frequently less than 15 min, instead of the threshold 15 min, and the field-aligned profile is also augmented with other beam azimuth and elevation angles in order to capture the horizontal transport of plasma and hence, the electric field as a vector. There are also optimizations in altitude profile soundings such that the E- and F-regions use different pulse codes. This in turn enables optimization in altitude resolution to be achieved. Perhaps the most significant data uncertainty improvement of these observations is that the electron density in the F-layer (N_e) is calibrated from the electron plasma line being observed by PFISR. This provides an absolute accuracy that is typically within $\pm 5\%$ when such measurements are available. For purposes of comparison with other measurements such as in-situ satellite, ionosondes, GPS TEC this makes PFISR N_e the absolute standard of density. Furthermore, because the observations are almost continuous over a year they are important for model validation and providing long-term well-calibrated electron densities for empirical ionospheric models.

3.1. Sample PFISR observations

The observations of the PFISR F-region are examined in this study and presented for community wide usage. In this section, 2 days are highlighted to provide a contrast between an ionospheric quiet and active day. Day 140, 20 May 2007, and day 144, 24 May 2007, are the quiet and active day with daily Kp sums of 12.7 and 32.0, respectively. On the active day the highest three hourly Kp value was a 6 $^-$. Fig. 1 shows the PFISR observations for these 2 days with the left and right panels being the quiet and active days. Four parameters are color-coded as a function of altitude and UT. They are line-of-sight (los) drift velocity, electron temperature, ion temperature, and logarithm base 10 of the electron density in the bottom to top panels. A single color key defines each parameter for both days. Although in this study

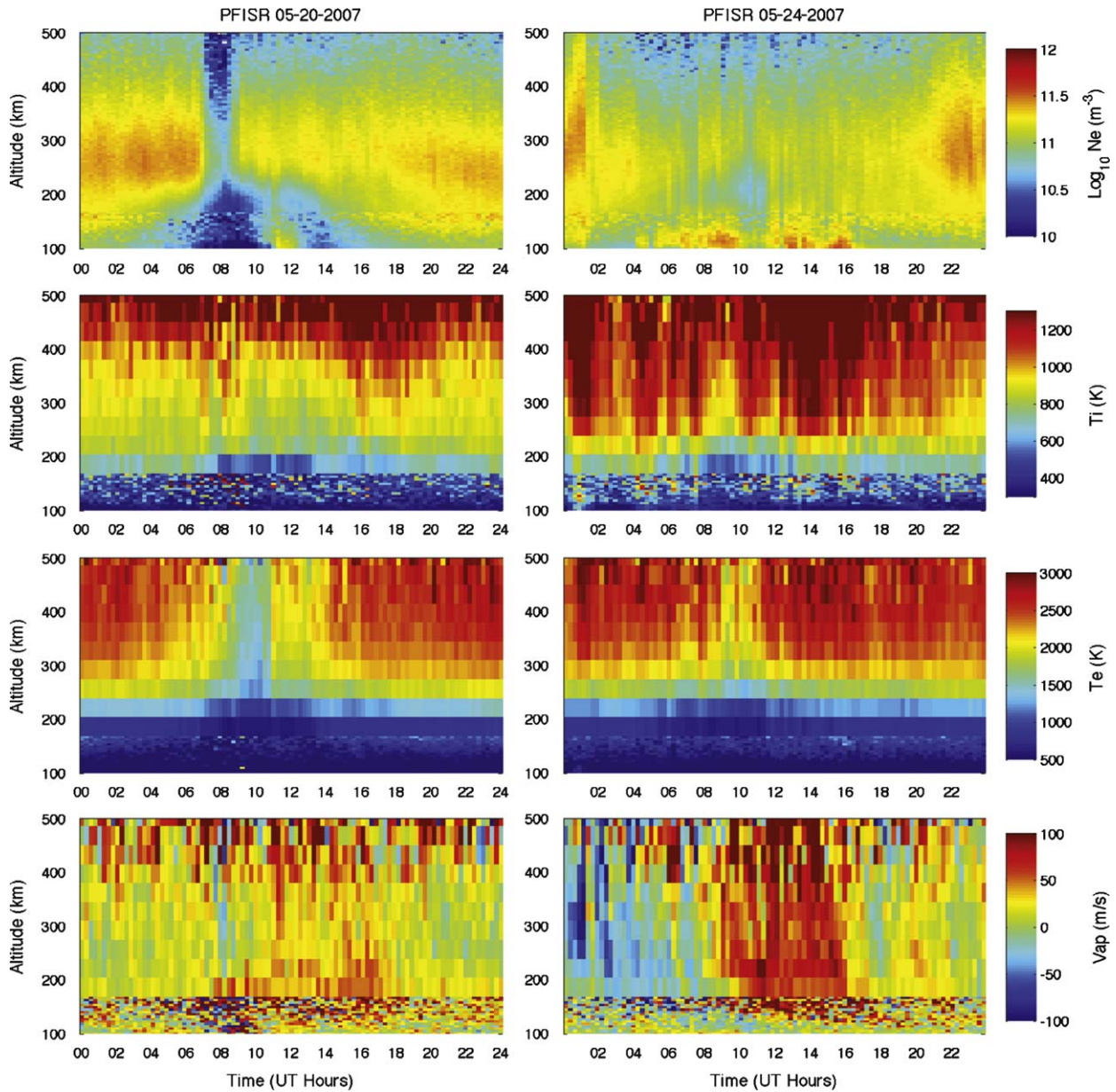


Fig. 1. PFISR IPY observations on 20 and 24 May 2007 in the left and right panels, respectively. The observations are LOS drift velocity, electron temperature, ion temperature, and logarithm base 10 of the electron density in the panels from bottom to top. Each parameter is color coded according to the color key on the right of their respective panels.

the emphasis is on the F-region, Fig. 1 includes the E-region observations.

The F-layer peak density shows a different character between the 2 days. On the quiet day the density profiles change relatively smoothly with time (left top panel), while on the active day the profiles change significantly in 15 min, which is the UT bin resolution shown in this plot. The term significantly refers to marked striations in the top right panel that correspond to many tens of percent to a factor of 2 change in density. Note this variability is not associated with plasma variability in a single flux tube over Poker Flat, but rather different flux tubes are convecting through the PFISR beam that have had different past histories. Hence, the perceived variability by comparing the quiet and active day describes spatial density irregularities over the high latitude and not local temporal variability. In the E-region the electron density between 100 and 150 km provide evidence of auroral precipitation that is occurring locally. An inspection of the E-region density structure and that of the F-region verify that

they are not strongly correlated confirming that the F-region density structures are not local temporal structures.

The ion temperature comparison, second panels from top of Fig. 1, provide a further marked difference between the 2 days. On the quiet day, left panel, the F-region around the density peak, 200–350 km, has a relatively small range of temperature variation over the 24 h period. The range is approximately 850 ± 200 K. In contrast the same altitude region on the disturbed day has temperatures as low as 800 K and over 1400 K with the temperature varying on time scales of fractions of an hour to a few hours. The ion temperature variability is not the same as found in the electron density variability. In the second from bottom panels, the electron temperatures are shown and they are found to be significantly hotter in the F-region, above 250 km, than the ion temperature. The electron temperatures are hottest at the highest altitudes with temperatures reaching and exceeding 3000 K at 800 km. These temperatures are typically 1500 K hotter than the corresponding ion temperatures, i.e., double the

T_i . Overall, the electron temperatures are hotter on the active day, are structured, but the structuring does not follow that of either the electron density or the ion temperature. Simple constant energy budget concepts expecting lower densities to be associated with higher electron temperatures do not apply.

The final parameter shown in the bottom panels of Fig. 1 is the LOS ion drift velocity. Drifts that are upwards along the beam, approximately up the local Parker Flat magnetic field line, are color-coded yellow to red and are positive velocities. On the active day a region at all F-region altitudes between about 1000 and

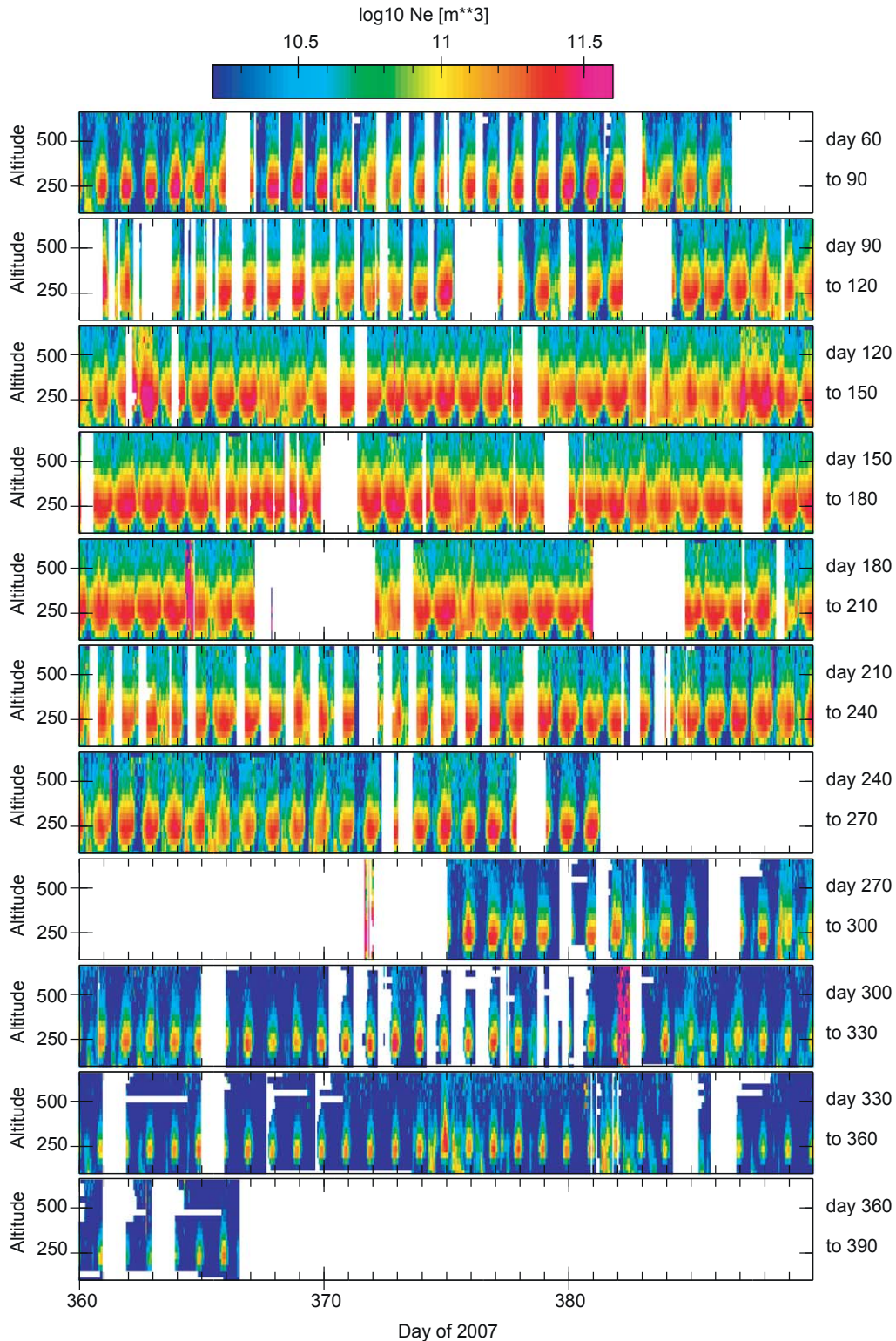


Fig. 2. PFISR electron density profiles from days 60–366 of 2007. Each panel is exactly 30 days long hence, approximately 1 month. Periods of no data are colored white. The logarithm base 10 density color key at the top of the figure has a maximum density of $2 \times 10^{11} \text{ m}^{-3}$. The range of days of the year for each panel are shown at the right side of each panel.

1600 UT are red. Note, Poker Flat has a geographic longitude of 212.53° East that corresponds to a 14.2 h UT offset from the solar local time (SLT). Hence this upward drift region is in the Poker Flat night sector. Given the days are in late May, the Poker Flat night is only a few hours long. The quiet day has a weakly upward drift during this time. On the quiet day the daylight hours show drifts that tend to be around zero, while on the active day between 0000

and 0800 UT there is a very distinct downward, light blue, ion drift. Since the observations are being made along the field line these drifts represent a combination of diffusion and neutral wind-induced drifts, but not $E \times B/B^2$ drifts. Given also the density and temperature measurements it will be possible to determine the strength of the neutral wind-induced drifts using models of the ionospheric physics.

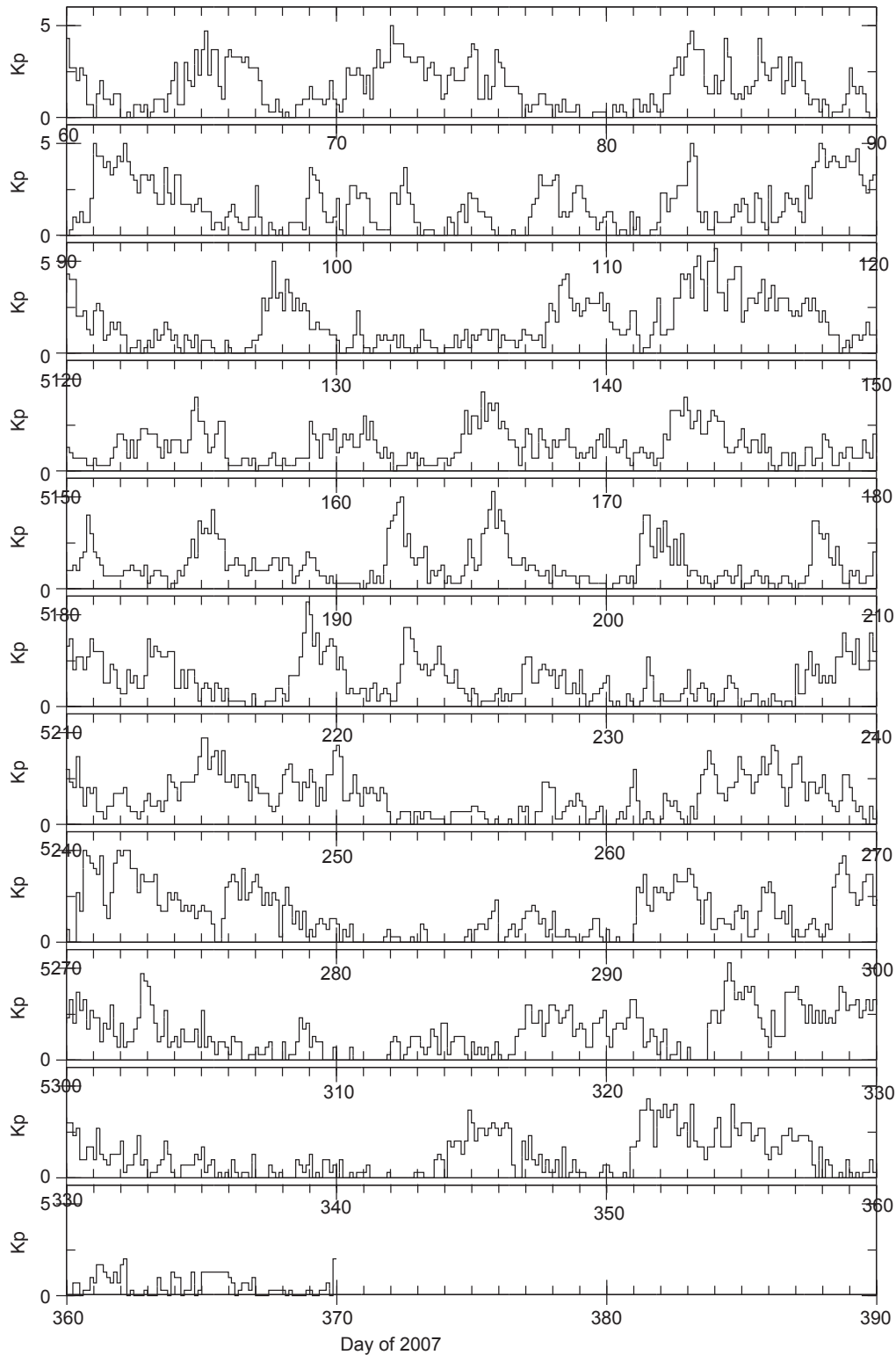


Fig. 3. Three hourly Kp index plotted in the same day of year format used in Fig. 2 to aid geomagnetic activity comparisons with the PFISR observations.

3.2. PFISR N_e through 1 January 2008

In Section 3.1, 2 days of PFISR observations were used to contrast quiescent and active day ionospheric conditions, in this section the entire IPY to date, through 1 January 2008, is presented as an overview. Fig. 2 shows the electron density as a function in altitude and day-of-year in 30-day panels between 1 March 2007 and 1 January 2008. Throughout this paper the day-of-year beginning on 1 January 2007 is used as the day indicator. The IPY began on day 60. Although not a complete year, the figure does span all four seasons during a solar minimum period. Specific daily details are not readily inferred from this plot, but the climate and weather tradeoffs are apparent. The white days in Fig. 2 represent times when PFISR was operating in incompatible modes or was off line. The long period from day 251 to about 284 was a period when PFISR was undergoing further hardware upgrades. In both the 60–90-day panel and those beyond day 270 there are also horizontal white strips. These represent situations when the ionospheric ISR echoes were not able to be analyzed probably because of the low densities.

The seasons are most readily tracked by the number of hours of darkness when the density falls by almost 2 orders of magnitude and is represented by a darkish blue color. The summer months almost see no such drop while equinox has on the order of 8–14 h and winter is just very dark blue almost all day. The Poker Flat geographic location of 67° places it at the latitude of darkness all winter day and sunlit all summer day. In turn, this extreme solar modulation with season inhibits the presence of the so-called Northern Hemisphere “seasonal anomaly”. This phenomena would be evidenced by higher F-layer densities in daytime winter than in summer, which is not observed in this data set. In fact, the summer densities appear to be highest, even denser than those at equinox.

The day-to-day variability, termed ionospheric weather is prevalent. This IPY study has as one of its objectives to associate this day-to-day variability with ionospheric drivers. Specifically, is it possible to establish how much of the variability is driven by the magnetosphere from above and how much is driven by the atmosphere from below? In this context a simple measure of magnetospheric variability would be the Kp index, although for more accurate tracking, the AE index would be superior since Poker Flat is an auroral location. However, the AE index is not yet available for the entire period of interest. Fig. 3 shows how Kp, the three hourly index varies over the same IPY time period as Fig. 2, in fact, in a format that can readily be compared to Fig. 2. The surprising aspect of Fig. 3 is that although this is solar minimum, there are continuous episodes of Kp disturbances up to and over 4. In fact, these episodes are almost “periodic” over a few to 10 days. At a first glance comparison these disturbances also occur during periods when the ionosphere exhibits significant day-to-day variability. Examples of this are readily seen, days 117–119, days 127 and 128, days 142–146, days 334–337, and others. In each case the identification of the variability in Fig. 2 is in how structured, in time, the N_e altitude profiles are along with the presence of E-region ionization. These variations are not adversely influenced by noise issues, but are tracking F-region electron density differences associated with the different plasma flux tubes that are $\mathbf{E} \times \mathbf{B}/B^2$ convecting through the PFISR beam. In fact, this variability represents a measure of the high-latitude ionospheric inhomogeneity. In Section 4 an analysis will be undertaken to determine how much of this weather can be associated with geomagnetic activity.

A comparison of Figs. 2 and 3 provide some overview inferences. Whenever Kp is active, above about 2, the peak electron density decreases, in Fig. 2 this is most readily identified with the noon N_mF_2 color going from red (high density) to yellow

(lower density). Good examples of this are days 70–74, 83–85, 99–103, 144–145, and 245–250. In addition, on some quiet days the dayside density appears to be particularly enhanced over adjacent similar quiet days. An example of this is day 122. This quiet day variability is particularly interesting and is the type of data to be studied during the IPY and post-IPY analysis period. The very evident Kp inverse influence/correlation with peak dayside electron density, although not a surprise, begs the question of why this was not a primary binning in empirical ionospheric models. Specifically the International Reference Ionosphere (IRI) model (Bilitza, 2001) does not have a geomagnetic dependence in how the data were binned to form the empirical model, rather observations were selected on a monthly central quartile method to exclude outliers that were presumed to be due to extremes in weather. IRI now has a semi-theoretical geomagnetic storm option to compensate for a storm extremes in weather (Araujo-Pradere et al., 2004). At mid-latitudes this Kp dependence is also a long since recognized trend (Papagiannis et al., 1975; Rishbeth et al., 2000).

4. A reduced PFISR IPY data set

The PFISR IPY database can be characterized by a reduced number of parameters such as the F-layer peak density and height, N_mF_2 and h_mF_2 , respectively. In this study the emphasis is on the F-layer, hence, the following four parameters are adopted for further study; N_mF_2 , h_mF_2 , T_i at 300 km, and T_e at 300 km. The ion temperature is chosen as an indication of energy input to the thermosphere as well as frictional heating of the ions, while the electron temperature is a relatively independent measure of the coupling to the magnetosphere above as well as electron precipitation via energy degradation of precipitating electrons at lower altitudes. At the altitude of 300 km, the coupling between T_i and T_e is relatively second order to their defined dependencies. Future studies will extend the analysis to include other altitudes, the Doppler drift velocity as well as the E-region observations.

4.1. Four-parameter PFISR IPY

Fig. 4 shows how the four parameters listed above and the daily Kp vary from 1 March 2007 to 1 January 2008. The Northern Hemisphere mid-summer lies around day 174 and mid-winter around day 359. In Fig. 4 these two times correspond to a distinct minimum and maximum variability in the N_mF_2 , second panel from the bottom. The variation is both a measure of day-to-day variability and the diurnal variation at Poker Flat. The ion temperature at 300 km, third panel from bottom, exhibits dramatic fluctuations, but of specific interest are the multi-day episodes when the minimum ion temperature increases. Examples of this are the 5 days around day 119 and around day 145. The ion temperature appears to have increased by up to 150 K over the earlier and later days. These same days have a marked increase in the sum of Kp, see top panel.

4.2. Days 114–126

To see this similarity more directly, Fig. 5 shows the 12 days beginning on 114 extending through 126 for the same information shown in Fig. 4. Now the diurnal variation becomes evident on all four parameters during quiescent conditions. For diurnal reference, local solar noon is marked by vertical arrows at the bottom of each panel. Hence, on quiescent days h_mF_2 has its lowest value near noon while N_mF_2 , T_e 300 km, and T_i 300 km all show a distinct minimum at midnight, which given that the season is

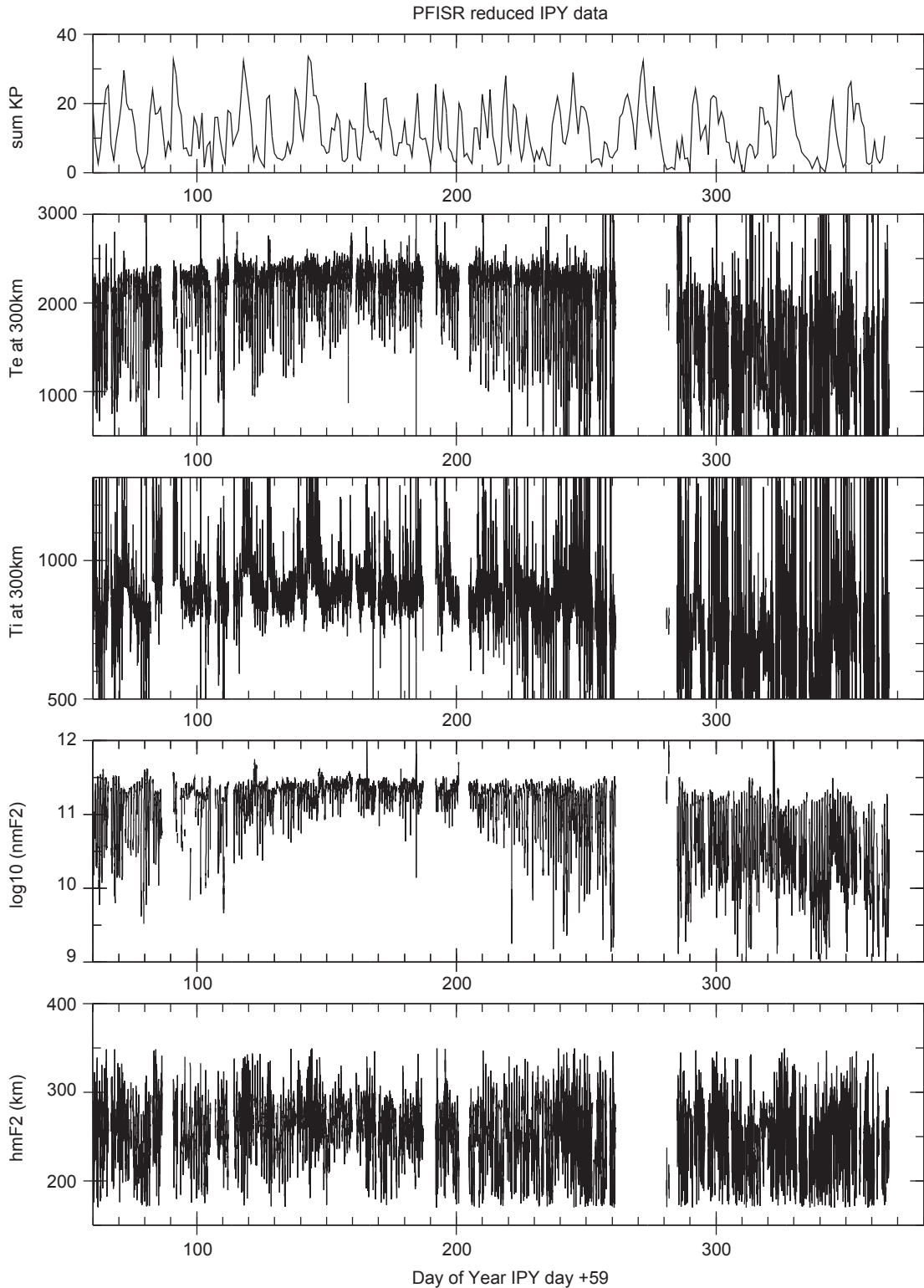


Fig. 4. PFISR reduced parameters, h_mF_2 , $\log_{10}N_mF_2$, T_i at 300 km, and T_e at 300 km plus the daily sum Kp in panels from bottom to top for the period days 60–367.

near mid-summer, corresponds to the few hours of darkness at Poker Flat. Both the h_mF_2 and T_i at 300 km do not show a diurnal variation during the 117–119-day period. This corresponds to when the daily sum of Kp was also elevated (see top panel, Fig. 5). This active T_i change in morphology evident in Fig. 5 for a specific disturbed period is in fact a common dependence for other disturbed periods, see Fig. 4. In neither of the other three parameters is there such a strong trend with the daily Kp value.

During these days the N_mF_2 diurnal pattern changes and in the daytime decreases are evident. Fig. 5 provides a graphic view of how quiescent and active days can be separated. In fact, this criterion of using smooth repeating diurnal variations in all four parameters, although subjective, has been applied to the entire IPY PFISR database. This then resulted in a surprising total of only 77 quiescent and 231 active days. The original campaign hope was that most of the days would be quiescent, i.e., devoid of

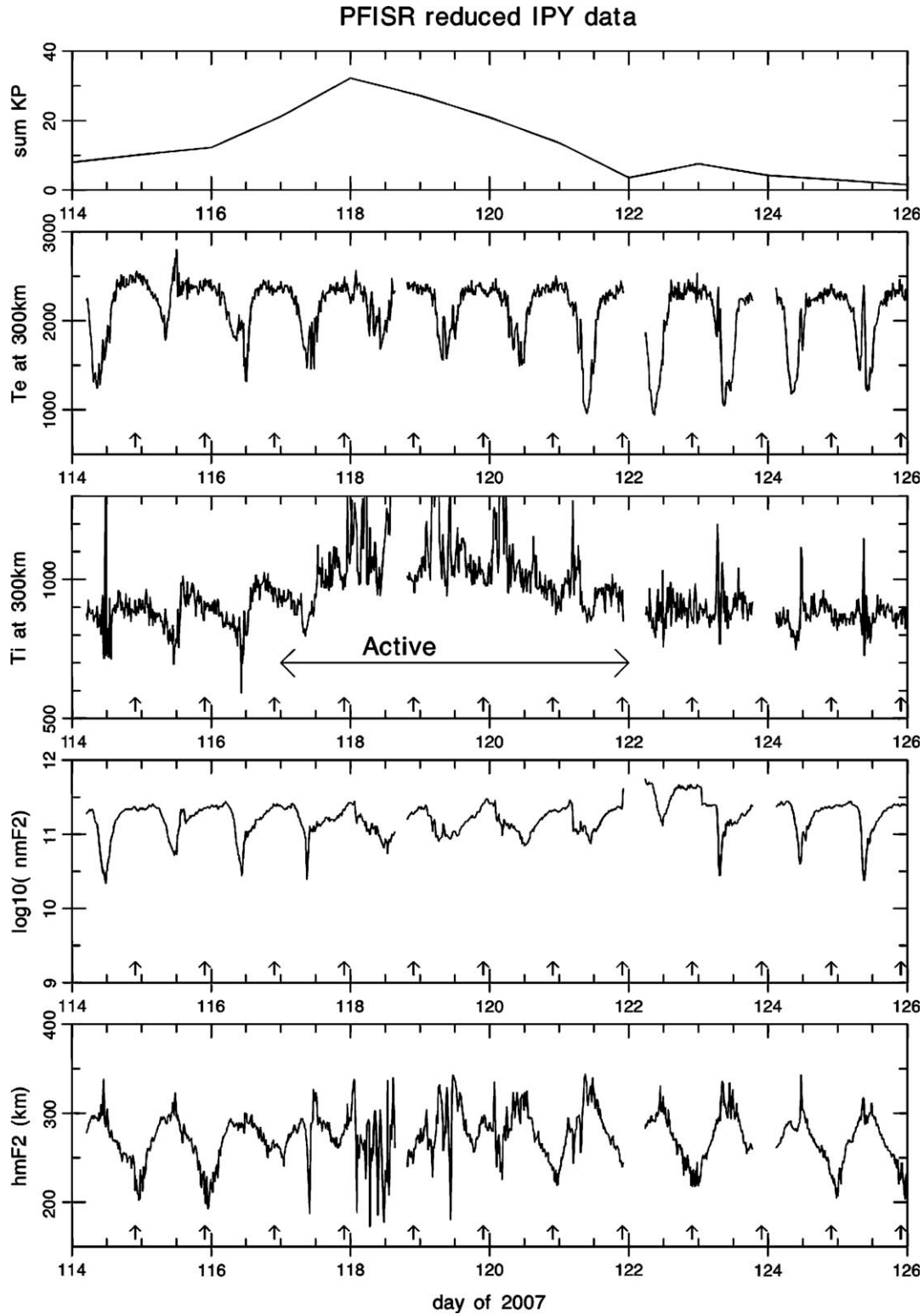


Fig. 5. PFISR reduced parameters; $h_m F_2$, $\log_{10} N_m F_2$, T_i at 300 km, and T_e at 300 km plus the daily sum Kp in panels from bottom to top for a 12-day period beginning on day 114 (24 April 2007). Local noon is marked by vertical arrows at the bottom of each panel.

geomagnetic activity hence, enabling the effects of atmospheric drivers from below to be easily identified in the IPY dataset.

4.3. Days 339–350

During winter marked trends following the Kp index are also evident. Fig. 6 shows PFISR-reduced parameters for the 12 days

beginning on day 339 (5 December 2007) in the same format as Fig. 5. Throughout the 12 winter days the $N_m F_2$, second bottom panel show a well-defined daytime peak density. Local noon is identified each day by the upward pointing arrows. These noon-time densities reach $2 \times 10^{11} \text{ m}^{-3}$ while the nighttime densities before day 344 are about $1 \times 10^{10} \text{ m}^{-3}$. During the geomagnetic disturbance beginning day 344–347 it is the nighttime density

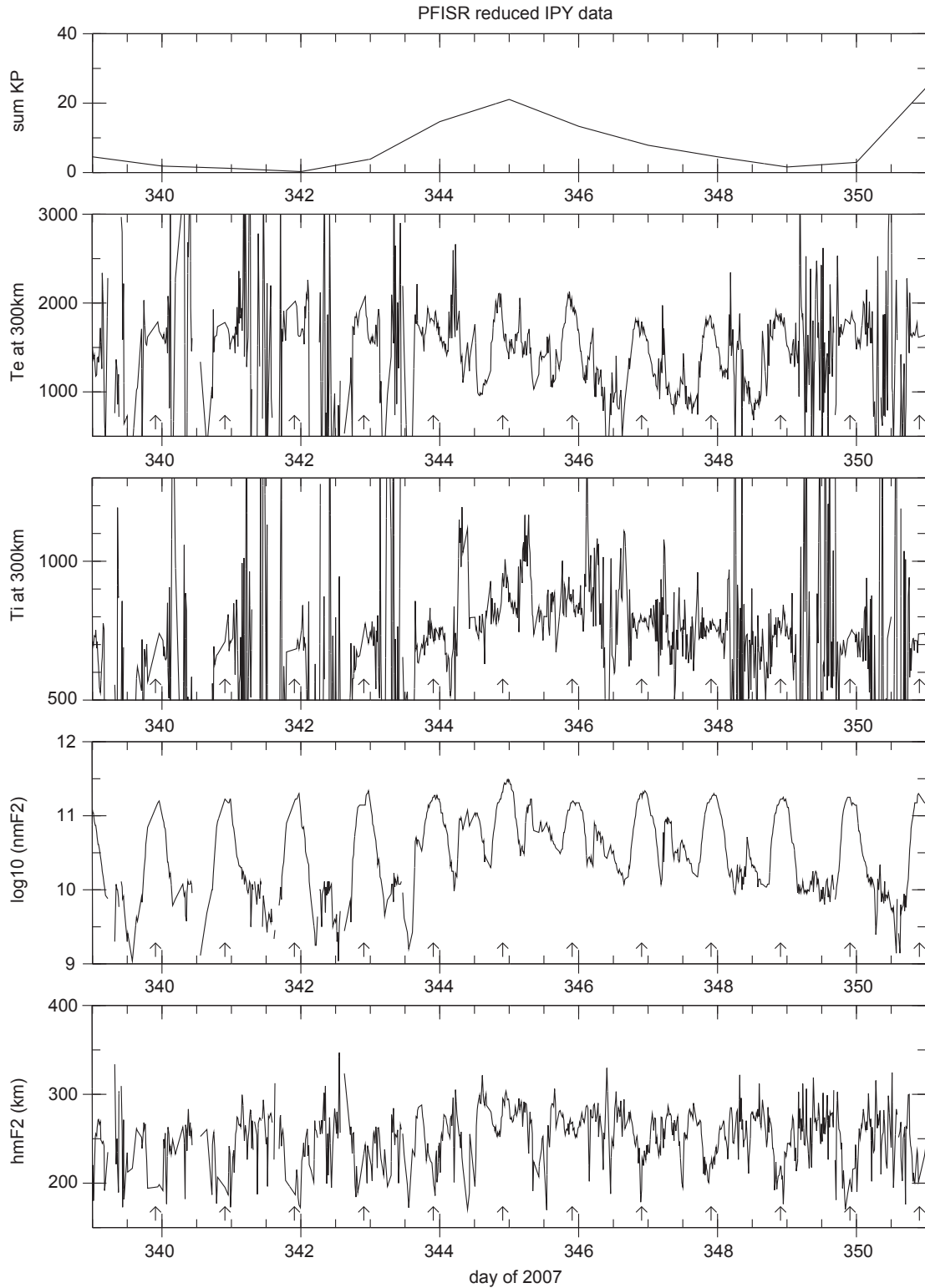


Fig. 6. PFISR reduced parameters, h_mF_2 , $\log_{10} N_mF_2$, T_i at 300 km, and T_e at 300 km plus the daily sum Kp in panels from bottom to top for a 12-day period beginning on day 339 (5 December 2007). Local noon is marked by vertical arrows at the bottom of each panel.

that increases to $1 \times 10^{11} \text{ m}^{-3}$ on days 345 and 346. These 2 days correspond to a time when the three hourly Kp value stayed above 2 but also mostly below 3. Hence, this was not a dramatic disturbance. Figs. 2 and 3 provide more detailed information on the electron density profile and the 3-h Kp index. In Fig. 2 on days 344, 345, and 346 show very marked nighttime E-region ionization, i.e., auroral precipitation and modified daytime

characteristics. Fig. 3 shows that during this 3-day period the 3 hourly Kp value was sustained at about 2.5. Returning to Fig. 6, a number of disturbance-related observations can be made:

- (1) The T_i at 300 km increased during the disturbance by over 100 K from values at or below 700 K.

- (2) The T_i increase was not limited to nighttime when aurora was present but also in the daytime.
- (3) The T_e at 300 km does not follow the T_i at 300 km morphology, but shows a distinct daytime max ranging from 1600 to 2000 K.
- (4) h_mF_2 normally has a daytime minimum ground local noon, but during the disturbance this is elevated from values around 200 km to above 250 km.

Note, during the quiescent nighttimes, days 339–343 and 348–350, the very low densities are causing severe challenges for the analysis algorithms as evidenced by the large variability observed in the T_e and T_i panels of Fig. 6. A follow-on analysis for specific case-study periods will be used to optimize these analysis solutions.

5. PFISR IPY weather and climate

The observations shown in Fig. 2 span four seasons as well as a range of geomagnetic activity ranging from a Kp of 0–6. Figs. 5 and 6 showed specific summer and winter examples of how the ionosphere responds to geomagnetic activity. In order to distinguish between climate and geomagnetic activity, the data are binned into four seasons and four levels of geomagnetic activity. From 1 March 2007 to 1 January 2008 a total of 18,491 PFISR IPY altitude profiles were measured. This averages out at 60 per day over the 308-day period. The four seasons were defined as winter being 45 days on either side of winter solstice and summer being 45 days on either side of summer solstice. Then both spring and fall include the days between winter to summer and summer to winter, respectively. For this initial season–local time–magnetic activity binning of the observations it was decided to use the daily planetary index, Kp sum, and keep each observational UT day intact. When auroral indices such as AE become available this coarse geomagnetic binning, with possible aliasing effects, could be revisited to examine if the auroral F-region is more strongly controlled by the auroral index, hence, auroral processes. Hence, the daily sum Kp was used rather than the 3 hourly Kp index. Then the four levels of activity were defined as:

- Level 1, Kp sum less than 8;
- Level 2, Kp sum less than 16 and greater or equal to 8;
- Level 3, Kp sum less than 24 and greater or equal to 16;
- Level 4, Kp sum greater or equal to 24.

Table 1 tabulates the percentage of the 18,491 profiles that fall into each of the season–activity bins. These percentages do not correspond to a specific fraction of the 308 days since the PFISR IPY observational mode is not uniform over the 308 days. For example, in Fig. 2 periods of many days when PFISR was in another mode or off line are evident as the white periods. These are not uniformly distributed over the IPY period. However, comparing the season total percentages show that the profiles are distributed as 17.2%, 21.3%, 36.7%, and 24.8% over winter, spring, summer, and fall, respectively. Activity levels are distributed as

Table 1
Percentage distribution of PFISR IPY profiles.

Season	Level 1	Level 2	Level 3	Level 4
Winter	8.50	3.74	3.88	1.06
Spring	8.03	4.86	6.07	2.34
Summer	13.41	13.82	7.06	2.36
Fall	9.07	7.34	7.40	1.05

39.0%, 29.8%, 24.4%, and 6.8% over levels 1, 2, 3, and 4, respectively. A 39% of the profiles were obtained for conditions of the daily run Kp being less than 8, an average 3 hourly Kp index of less than 1. However, 54.2% of the profiles had average 3 hourly Kp values between 1 and 3.

5.1. T_i at 300 km weather and climate

The ion temperature at 300 km is found to have the most systematic variation of the four reduced parameters. In fact, this parameter provides a link to the thermosphere and the Joule heating process. Hence this parameter probably will provide the greatest constraint on ionospheric–thermospheric (I–T) models. Fig. 7 shows all 16 combinations of season and activity level with each being represented by a panel showing the T_i at 300 km as a function of solar local time (SLT) at Poker Flat. Around noon the T_i at 300 km has a well-defined trend in both season and activity. Summer has higher temperatures than spring and fall, which both have a higher temperature than winter. Then T_i at 300 km increases as activity level increases. The winter to summer T_i temperature increase at activity level 1 is between 100 and 200 K. This is about the same range of T_i temperature increase from activity levels 1–4. At night in winter the low densities challenges the T_i analysis and as seen in Fig. 7, left column of panels, the night T_i is variable over at least the 500–1300 K plot limit. These data would need to be reanalyzed before further use is made of them. For many of the panels the nighttime T_i are less variable and tend to show values that are elevated over the daytime values. This is especially the case as activity level increases. Hence, this is likely associated with enhanced convection and Joule heating, on specific days. Both Figs. 5 and 6 provided evidence that the T_i at 300 km response to activity was very systematic on a case-by-case basis. Hence, although each panel in Fig. 7 shows a significant statistical spread, there is underlying coherence in the ionospheric response.

5.2. $\log_{10} N_mF_2$ weather and climate

Fig. 8 shows for all 16 combinations of season and activity how the F-region peak density, N_mF_2 , varies with solar local time. The N_mF_2 is plotted as a logarithm to the base 10 to enable its day–night dynamic range to be captured. In summer this variability is very small, see the summer column, while in winter at level 1 the night N_mF_2 values drop to a few times 10^9 m^{-3} while at noon they reach $2 \times 10^{11} \text{ m}^{-3}$. As activity level increases, the winter night densities systematically increase while the noon show a measurable decrease with activity. In summer there is almost no day or night activity trend visible. At equinox, both the spring and fall, the night densities tend to increase with activity while at noon no clear trend is evident.

5.3. h_mF_2 weather and climate

Fig. 9 following the earlier Figs. 7 and 8 format provides the solar local time variation of h_mF_2 , the F-layer peak height. For low activity levels there is a well-defined minimum, maximum h_mF_2 around noon. At the level 1 case this noon maximum value of h_mF_2 is highest in summer and lowest in winter, i.e., 255 km compared to 225 km. For each season this maximum noon h_mF_2 value increases with activity. For the level 4 panels, top row of Fig. 9, when the daily Kp sum exceeded or equaled 24 the h_mF_2 appears both “noisy” and also relatively similar all day long, i.e., the noon minimum is no longer present. Note, the wide range of variability of the h_mF_2 , level 1, noon-time hours will probably decrease as more sophisticated h_mF_2 fitting algorithms are applied to the

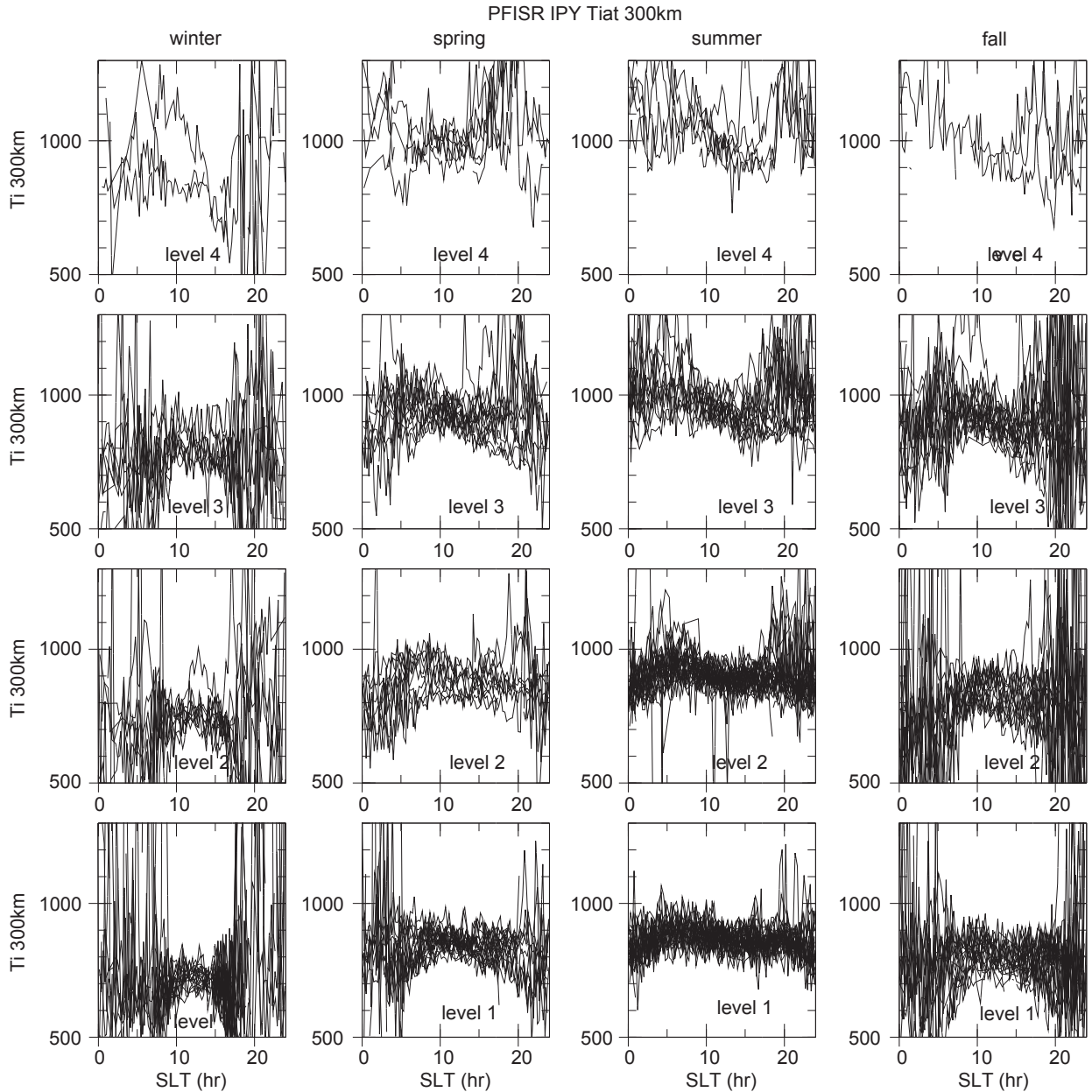


Fig. 7. Daily PFISR IPY T_i at 300 km sorted according to season and activity level plotted as a function of solar local time. Seasons are defined as 45 days before and after solstice, while activity level is based on the daily Kp run, see text. Seasons winter, spring, summer, and fall corresponds to the columns going left to right. Activity levels 1 (quietest), 2, 3, and 4 (most disturbed) correspond to the rows from bottom to top.

electron density profiles. In Fig. 2, the altitude profiles of N_e appear very systematic, however, the E- and F-region PFISR IPY modes have different pulse schemes and the transition altitude lies at 150 km. This altitude does come close to the noon, low activity level, $h_m F_2$ values seen in Fig. 9.

5.4. T_e at 300 km weather and climate

Fig. 10 provides the solar local time variation of T_e at 300 km over the 16 combinations of season and activity level. Daytime T_e is larger than night and summer is warmer than winter. T_e , however, does not follow the same trends that T_i has. Summer noon T_e ranges from 2200 to 2300 K while the corresponding T_i values are 800–1100 K. At night the T_e value decrease markedly down to values around 1000 K. In sharp contrast the T_i values either stay similar to the day values or are increased at night. This

is especially the case as activity level increases. A good example of this is to compare Fig. 7 T_i with Fig. 10 T_e in summer, for each corresponding activity level.

6. Discussion

The IPY period does contain a large number of days with moderate geomagnetic activity. In the first 10 months presented here 54% of the observations were made with daily average three hourly Kp between 1 and 3. Although not storm level, these periods, often extending over more than a day, have very measurable impact most readily seen in the ion temperature. This raises a different way of comparing with models. Usually ionospheric model data comparisons focus on the electron density, either getting $N_m F_2$, or TEC, or layer height correct. Although this is still true for the IPY database, a more restrictive requirement

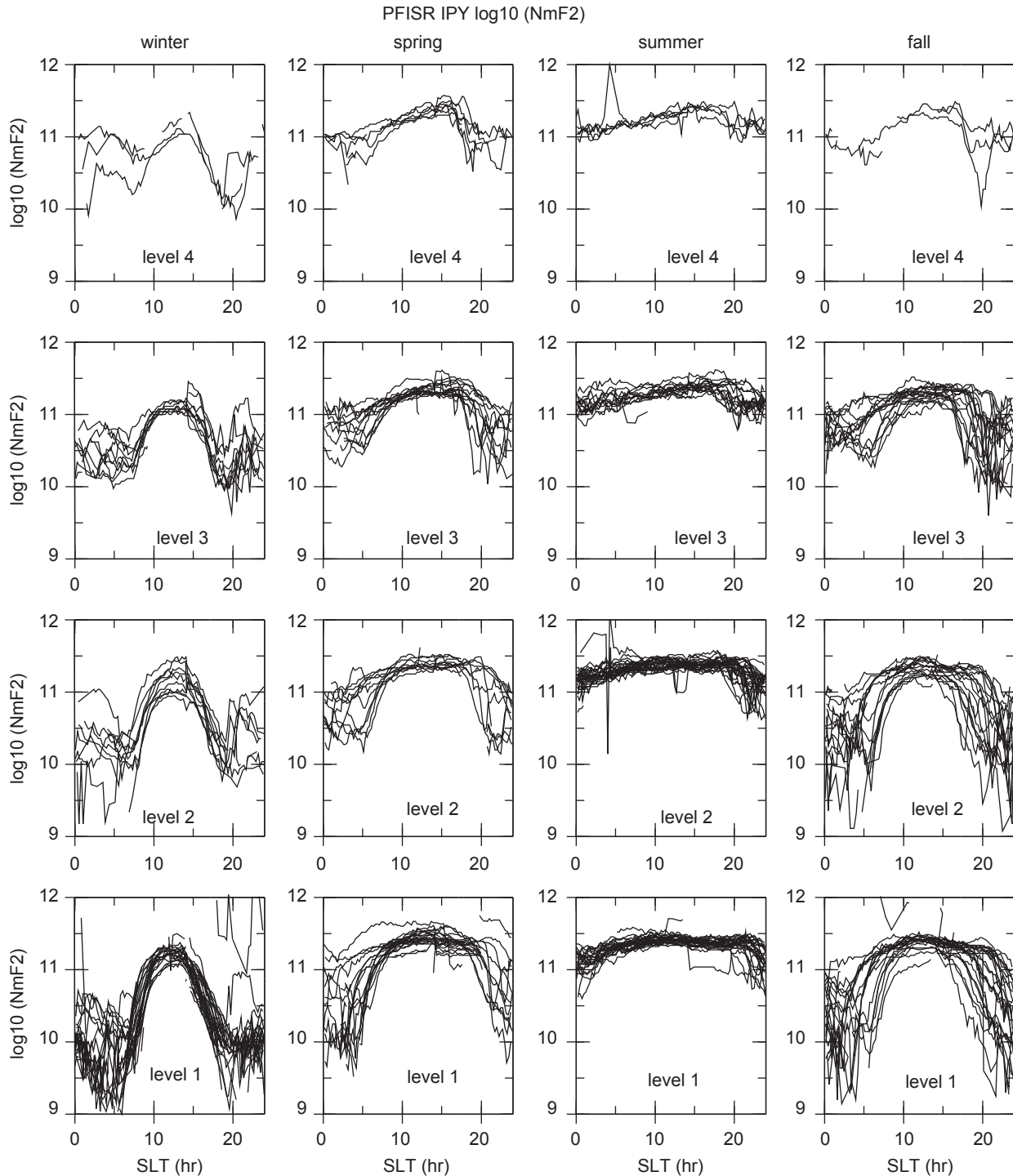


Fig. 8. Daily PFISR IPY $\log_{10} N_e$ sorted according to season and activity level in the same format as Fig. 7.

will be that the model's energy equation solutions for both T_i and T_e can be tested. Hence, the unique focus of such model data comparison need to focus on the temperature as well as density over long periods of climate and weather. Present day ionospheric modeling can be divided into at least three categories each would make use of the IPY data set in a different way. These categories are: real-time specifications of weather; physics models to study ionospheric processes; and empirical models to forecast long-term trends, i.e., seasonal and solar cycle.

In the cast of real-time specification models, e.g., the CTIPe run in real-time at the Space Weather Prediction Center (SWPC) or the

USU-GAIM model run at the Air Force Weather Agency (AFWA) the models use indices and data available in real-time. These ionospheric specifications then include ionospheric weather as well as longer term climate trends. Validation of these specifications requires independent observations of the specified parameters over long periods such that weather-climate trends can properly be accounted for. A problem with short period data sets is that identifying whether the models climate or weather processes are responsible for mismatches to observations is left as an open question. Hence, long data sets that span seasonal climate changes, e.g. the IPY data set, does provide a resolution to this

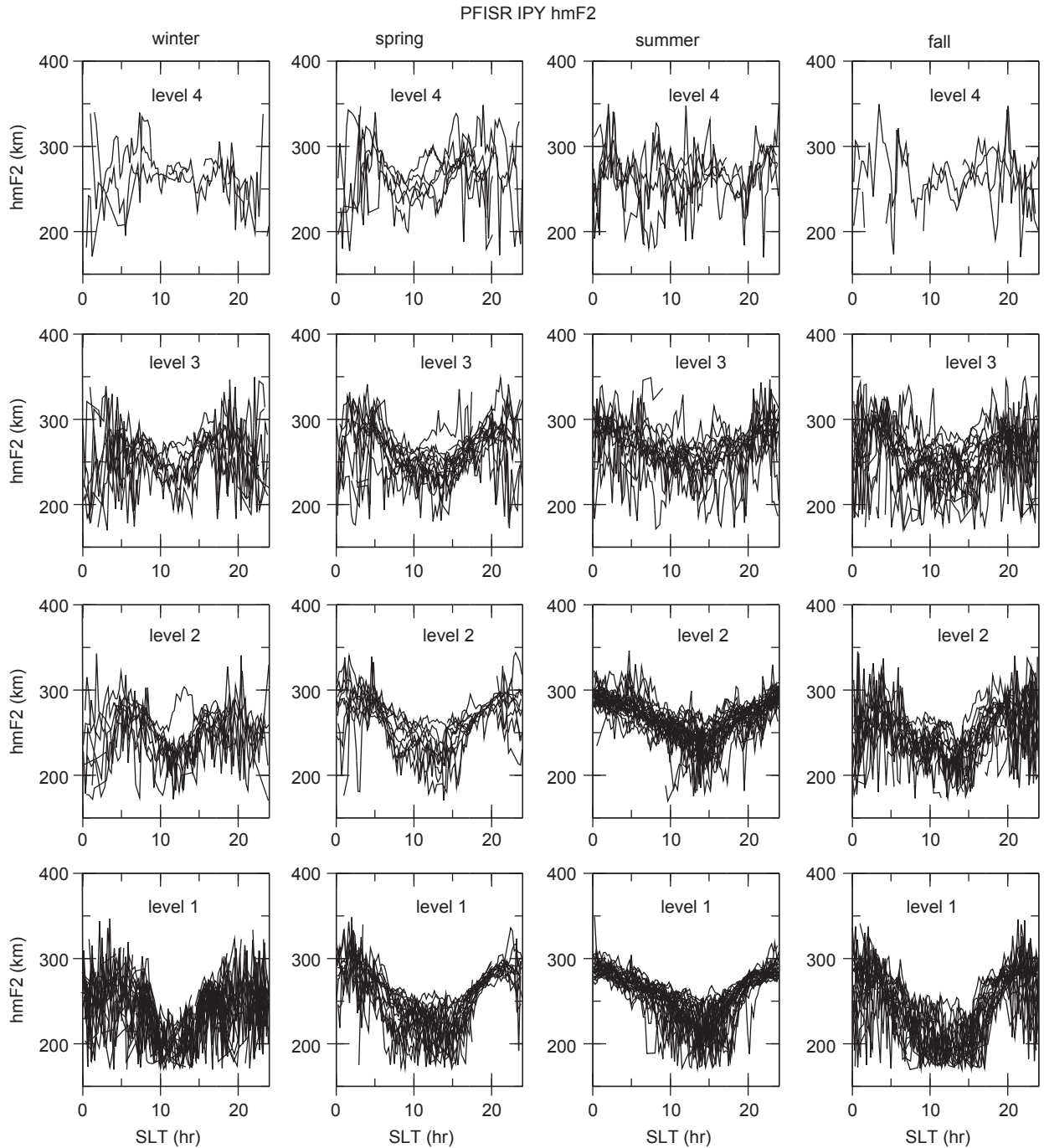


Fig. 9. Daily PFISR IPY h_mF_2 sorted according to season and activity level in the same format as Fig. 7.

long standing validation issue. In addition, as already pointed out, the full ion and electron profiles essentially lock down the freedom the models have in setting boundary condition on the energy equations that they solve. The long-term IPY data set could potentially become the basis for a comprehensive skill score analysis for real-time ionospheric models. Sojka et al. (2007b) used 1 month of ionosonde observations in Australia to study how a skill score could be developed using ionospheric specifications generated by the USU-GAIM-Gauss Markov. Their study found that even 1 month of observations does not clearly establish the climate baseline to which weather either adds or detracts. A somewhat ideal use of IPY PFISR-like observations would be to directly assimilate them into a real-time assimilation model such

as the USU-GAIM. However, at this time the challenges in bringing this to fruition are immense.

The physics model studies would enable comparisons of their ionospheric output to be made with the IPY database to reveal strengths and weaknesses in these models. Being research grade models they have a relatively large number of processes that can be validated, or simply adjusted. Anderson et al. (1998) showed how this process provides both validation and at the same time insight into physical mechanism embedded in the models that are important to the model outcome. Their study only used a few isolated days of observation and hence has the problem of distinguishing between climate and weather. Recently it has become apparent that during the IPY period although the Sun was

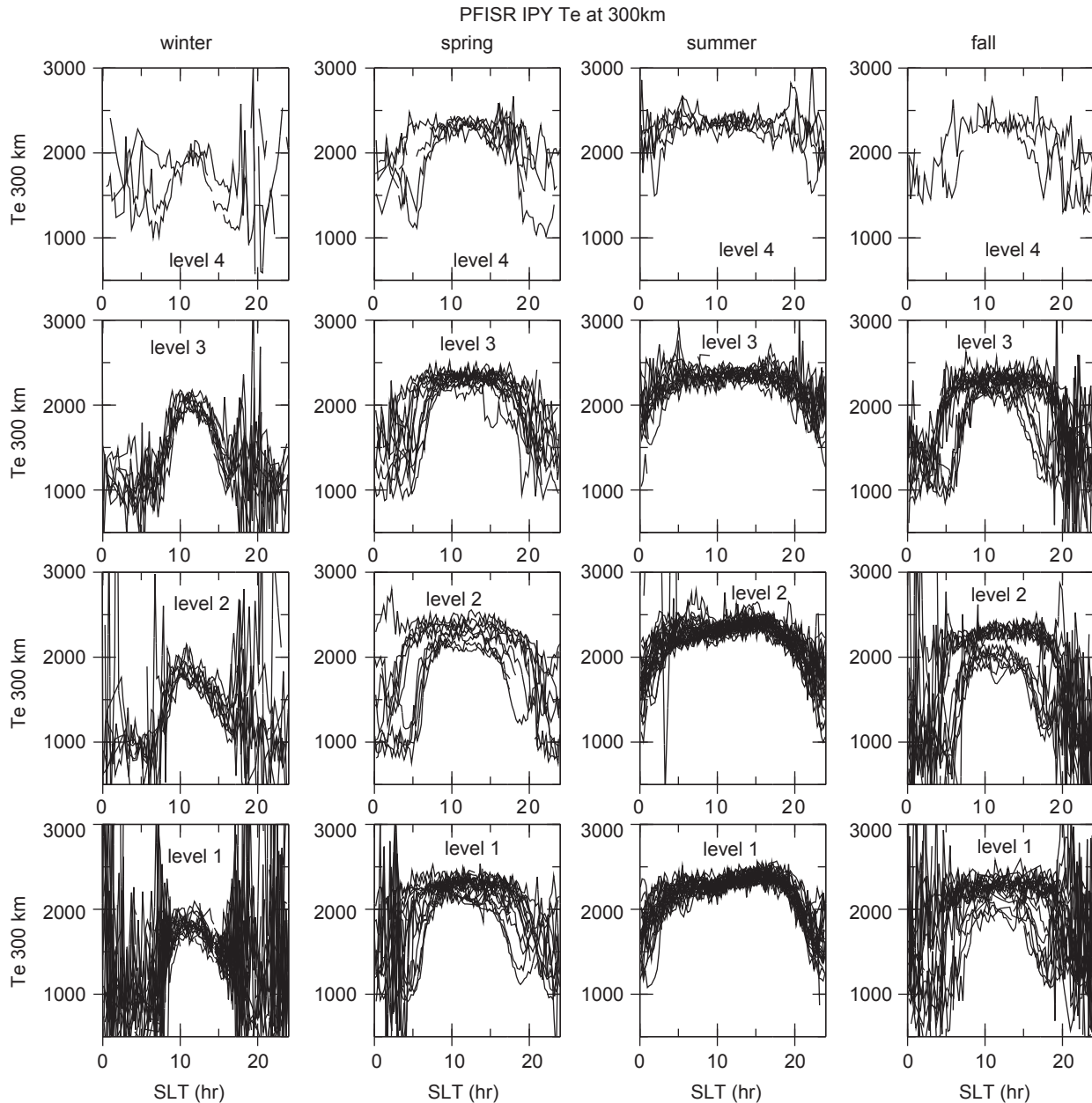


Fig. 10. Daily PFISR IPY T_e at 300 km sorted according to season and activity level in the same format as Fig. 7.

in a solar minimum state the fast solar wind streams associated with coronal holes swept across the geospace environment with a period of about 9–10 days. In turn the magnetosphere–ionosphere system becomes energized with sustained non-classic substorm activity for many days at a time (Kozyra, 2008, private communication). Although this phenomena is not new the continuous observations in the auroral zone by the PFISR will provide a key estimate of how energy is being deposited in the thermosphere–ionosphere system. Hence, the ionospheric mode-IPY PFISR analysis will need to emphasize how the magnetosphere–ionosphere electrodynamic operates during these fast stream recurrent events. Ionospheric drivers for such events currently either do not exist or are in a conceptual state.

The comprehensive nature of the PFISR IPY observations through both the E- and F-regions will also provide a unique polar solar minimum database for empirical modeling that emphasize climate. The International Reference Ionosphere (IRI) is the standard for such modeling. However, even so its

description of the temperatures is limited due primarily to the historically sparse number of such measurements. The PFISR data set provide complete altitude profiles of both T_e and T_i during both quiet and moderate geomagnetic activity over all four seasons. In Section 5 the statistical binning by season and geomagnetic activity shows that the geomagnetic control of T_i at 300 km, Fig. 7, was as large as that of season. Hence, the IPY observations have unique contributions for empirical modeling of the ionosphere where the main customers are the application and forecast community.

The PFISR IPY data set has a twin. The EISCAT Svalbard Radar (ESR) located in the polar cap at Longyearbyen has also been operating “continuously” with an equivalent mode since 1 March 2007. These two data sets provide complementary views of ionospheric plasma inside the polar cap and in the auroral region. Although located at quite different locations, there are times of the day at which plasma seen at one location could well be transported to be seen at a later time at the other. A key to

understanding this polar connectivity will come from global convection patterns that can be obtained from the Assimilative Mapping of Ionospheric Electrodynamics (AMIE) or from Super-DARN convection patterns. In either case, one of the major model studies to be undertaken is the polar ionospheric simulation using the best available convection patterns in order to simultaneously compare to PFISR and ESR. This study would also provide the polar Joule heating input that probably is being monitored by the PFISR T_i at 300 km during periods of quite moderate geomagnetic activity, see Figs. 5 and 6.

7. Summary

The PFISR IPY experiment continues to operate as the IPY first 17 months is reached at the time this article is being written. The experiment mode has been augmented with the addition of light-of-sight measurements to provide information on the auroral electric fields at Poker Flat. Over the first 10 months presented here a number of scientific and operational results and uses can be expected:

- The almost continuous observations over all four seasons will enable resolution of present day model comparisons with short data sets where problems associate with weather and climate cannot be resolved.
- Similarly establishing how boundary conditions should be set on the solutions for both the ion and electron energy equation will be enabled by the long data sets that clearly distinguish between climate and weather.
- Because these observations provide a very good, accurate, density both in magnitude and altitude profiles they are particularly important as a reference for ionospheric model skill score development.
- These same attributes provide new observational attributes for consideration in empirical ionospheric modeling. Specifically a geomagnetic control dependence and both profiles of electron and ion temperature at solar minimum over season, local time, and geomagnetic activity.

These observations are available to the scientific community and through a NSF CEDAR working group will form the basis for community participation in model-observation comparisons at

high latitudes. Through this, CEDAR working group observations from other ISRs as well as other ground-based and satellite measurements will be coordinated. As mentioned in Section 6, the convection patterns become a key ingredient to establishing the polar ionospheric distributions and hence are complementary observations needed by the models. For participation in this CEDAR IPY working group, contact the authors.

Acknowledgments

This research was supported by NSF Grant ATM-0408592 to Utah State University. PFISR is operated by SRI International under NSF Cooperative Agreement ATM-0608577.

References

- Anderson, D.N., et al., 1998. Intercomparison of physical models and observations of the ionosphere. *Journal of Geophysical Research* 103, 2179–2192.
- Araujo-Pradere, E.A.T., Fuller-Rowell, J., Bilitza, D., 2004. Time empirical ionospheric correction model (STORM) response in IRI2000 and challenges for empirical modeling in the future. *Radio Science* 39, IS24A.
- Bilitza, D., 2001. International reference ionosphere 2000. *Radio Science* 36, 261–276.
- Dougherty, J.P., Farley, D.T., 1960. A theory of incoherent scattering of radio waves by a plasma. *Proceedings of the Royal Society of London* 259 (1296), 79–99.
- Evans, J.V., 1979. Theory and practice of ionosphere study by Thomson scatter radar. *Proceedings of the IEEE* 57 (4), 496–530.
- Heinselman, C.J., Nicolls, M.J., 2008. A Bayesian approach to electric field and E-region neutral wind estimation with the Poker Flat Advanced Modular Incoherent Scatter Radar. *Radio Science* 43, RS5-13, doi:10.29/2007/RS003805.
- Lehtinen, M.S., Haggstrom, I., 1987. A new modulation principle for incoherent scatter measurements. *Radio Science* 22, 625–634.
- Papagiannis, M.D., Hassan-Hosseini, H., Mendillo, M., 1975. Changes in the ionospheric profile and the Faraday factor M with K_p . *Planetary and Space Science* 23, 107–113.
- Rishbeth, H., Sedgemore-Schulthess, K.J.F., Ulich, T., 2000. Semiannual and annual variations in the height of the ionospheric F2-peak. *Annales Geophysicae* 18, 285–299.
- Schunk, R.W. (Ed.), 1996. *Solar-Terrestrial Energy Program (STEP): Handbook of Ionospheric Models*. Utah State University.
- Showen, R.L., 1979. The spectral measurement of plasma lines. *Radio Science* 14 (3), 503–508.
- Sojka, J., Schunk, R., van Eyken, T., Kelly, J., Heinselman, C., McCready, M., 2007a. Ionospheric challenges of the International Polar Year. *Eos Transactions, AGU* 88 (15), 171.
- Sojka, J.J., Thompson, D.C., Scherliess, L., Schunk, R.W., Harris, T.J., 2007b. Assessing models for ionospheric weather specifications over Australia during the 2004 climate and weather of the Sun–Earth–System (CAWSES) campaign. *Journal of Geophysical Research* 112, A09306.